



## Article

# Eudragit<sup>®</sup> L100/Polyvinyl Alcohol Nanoparticles Impregnated Mucoadhesive Films as Ocular Inserts for Controlled Delivery of Erythromycin: Development, Characterization and In Vivo Evaluation

Shahla Mirzaeei <sup>1,2,\*</sup> , Shiva Taghe <sup>2,3</sup>, Raid G. Alany <sup>4,5</sup> and Ali Nokhodchi <sup>6,\*</sup>

- <sup>1</sup> Nano Drug Delivery Research Center, School of Pharmacy, Kermanshah University of Medical Sciences, Kermanshah 6715847141, Iran
  - <sup>2</sup> Pharmaceutical Sciences Research Center, School of Pharmacy, Kermanshah University of Medical Sciences, Kermanshah 6715847141, Iran
  - <sup>3</sup> Student Research Committee, School of Pharmacy, Kermanshah University of Medical Sciences, Kermanshah 6715847141, Iran
  - <sup>4</sup> Drug Discovery, Delivery and Patient Care Theme, Faculty of Science, Engineering and Computing, Kingston University London, Penrhyn Road, Kingston upon Thames KT1 2EE, UK
  - <sup>5</sup> School of Pharmacy, Faculty of Medical and Health Sciences, The University of Auckland, Private Bag 92019, Auckland 1142, New Zealand
  - <sup>6</sup> Pharmaceutics Research Laboratory, School of Life Sciences, University of Sussex, Brighton BN1 9QJ, UK
- \* Correspondence: shahlamirzaeei@gmail.com (S.M.); a.nokhodchi@sussex.ac.uk (A.N.);  
Tel.: +98-833-426-6780 (S.M.); +44-12-7367-2811 (A.N.)



**Citation:** Mirzaeei, S.; Taghe, S.; Alany, R.G.; Nokhodchi, A. Eudragit<sup>®</sup> L100/Polyvinyl Alcohol Nanoparticles Impregnated Mucoadhesive Films as Ocular Inserts for Controlled Delivery of Erythromycin: Development, Characterization and In Vivo Evaluation. *Biomedicines* **2022**, *10*, 1917. <https://doi.org/10.3390/biomedicines10081917>

Academic Editor: M. R. Mozafari

Received: 28 June 2022

Accepted: 3 August 2022

Published: 8 August 2022

**Publisher's Note:** MDPI stays neutral with regard to jurisdictional claims in published maps and institutional affiliations.



**Copyright:** © 2022 by the authors. Licensee MDPI, Basel, Switzerland. This article is an open access article distributed under the terms and conditions of the Creative Commons Attribution (CC BY) license (<https://creativecommons.org/licenses/by/4.0/>).

**Abstract:** The fast elimination of drugs from the cornea is one of many challenges associated with the topical administration of conventional dosage forms. The present manuscript aimed to prepare modified-release inserts containing erythromycin (ERY) to enhance drug delivery and address the aforementioned limitation. Film formulations were developed using Eudragit<sup>®</sup> L100 (EUD) and Polyvinyl Alcohol (PVA) polymers. ERY-loaded EUD-based nanoparticles were developed by the colloidal dispersion method using PVA as the emulsifier. The film-casting method was applied to form the mucoadhesive films using sodium alginate, gelatin, cyclodextrin- $\alpha$ , and  $\beta$  as polymeric film matrices. Different physicochemical properties of the optimized formulations and in vitro release profiles were evaluated. The in vivo evaluation was performed by collecting tear samples of rabbits using a novel, non-invasive method following the administration of inserts in the cul-de-sac. The ERY amount was assayed using a microbiological assay. The developed films showed prolonged in vitro and in vivo release profiles over five to six days; they had suitable physicochemical properties and a tensile strength of 2–3 MPa. All formulations exhibited antibacterial efficacy against *E. coli* and *S. aureus* with more than 20 mm diameter of inhibited growth zones. None of the formulations caused irritation to the rabbit's eye. The inserts showed promising pharmacokinetics with AUC<sub>0–120</sub> of 30,000–36,000  $\mu\text{g}\cdot\text{h}/\text{mL}$ , a C<sub>max</sub> of more than 1800  $\mu\text{g}/\text{mL}$  at 4 h, and maintained drug concentration over the threshold of 5  $\mu\text{g}/\text{mL}$  during the following 120 h of study. Nanoparticle-containing, mucoadhesive films could be fabricated as ocular inserts and can prolong the topical ocular delivery of ERY.

**Keywords:** controlled-release; erythromycin; Eudragit<sup>®</sup> L100; mucoadhesive films; nanoparticles; ocular drug delivery

## 1. Introduction

Novel drug delivery systems (NDDS) such as vesicles, nanoemulsions, nanofibers, and nanoparticles have been shown to act as efficient carriers for the topical ocular administration of different drugs [1,2]. These systems are capable of overcoming many challenges and limitations associated with the administration of conventional topical eye drops. Poor drug ocular bioavailability is characteristic of simple aqueous solution eye drops where

rapid and extensive drug loss happens due to tear dilution, blinking, nasolacrimal drainage, pulse entry, metabolism, and non-specific absorption [3,4]. It has been shown that NDDSs may enhance the water-solubility of lipophilic drugs and prolong the amount of their time on the ocular surface by virtue of their mucoadhesive nature and ability to promote sustained drug release [5–7]. Previous studies have demonstrated the efficacy and benefits of these systems for ocular delivery of antibacterial, antifungal, and anti-inflammatory agents [8–10].

Polymeric nanoparticles (PNPs) that are classified as nanocapsules and nanospheres have attracted the attention of researchers in the past few decades [11]. These systems are drug-containing polymeric matrices with particle sizes ranging from 10 to 1000 nm [11]. PNPs have a wide range of applications in various fields, especially in drug delivery [12]. PNPs have the advantages of promoting drug controlled release, prolonging residence time, targeting the drug to the site of action, and consequently reducing side effects and enhancing drug absorption [13]. In addition to these advantages, PNPs can improve the bioavailability of drugs in the eye without causing blurred vision upon ocular administration. They can overcome the ocular barriers and improve the penetration of the drug through the cornea [14,15]. Mucoadhesive films can prolong the drug residence time on the surface of the eye, resulting in enhanced ocular bioavailability. By loading the mucoadhesive films with nanoparticles, the advantages of both of these systems can be realized [16–18].

Erythromycin (ERY) is a macrolide antibiotic that has an antibacterial effect on both gram-positive and some gram-negative bacteria [19]. The main mechanism behind ERY's antibacterial effect is the inhibition of protein synthesis by binding to the ribosomal peptidyl transferase of bacteria [20]. It was reported that ERY topical ocular ointment could prevent eye disease caused by methicillin-resistant *Staphylococcus aureus* [21,22]. Despite the wide-spectrum antibacterial effects, the conventional ERY ointment suffers poor patient compliance due to the need for frequent administration [23]. Hence, designing a prolonged-release delivery system is important to achieve a therapeutic level with less frequent administration.

A literature survey revealed that there are a limited number of studies aimed at developing an effective system for the improved ocular delivery of ERY. In a recent study, ERY-loaded nanostructured lipid carriers showed a prolonged release of 24 h with an enhanced corneal permeation [24]. In another study, a prolonged release of ERY (8 h release) was also observed from an in situ ocular gel formulation [25]. In a recent study, ocular inserts of ERY were fabricated and evaluated, and the results showed that the developed formulations can release ERY for 3 h [26]. To the best of our knowledge, the present study is the first to report on an ocular film prepared by a solvent-casting method that is intended for the ocular administration of ERY.

In the present study, mucoadhesive films loaded with nanoparticles were designed and developed using the biocompatible polymers Eudragit<sup>®</sup> L100 (EUD) and polyvinyl alcohol (PVA) for topical ocular delivery of ERY. The optimized formulations were evaluated for different physicochemical and mechanical properties. The efficacy of formulations to achieve sustained drug release as well as the improved antibacterial effect was demonstrated with the aid of in vivo and in vitro studies.

## 2. Materials and Methods

### 2.1. Materials

Sodium alginate (ALG), cyclodextrin- $\alpha$  and  $\beta$  (CD- $\alpha$  and  $\beta$ ), gelatin (GEL), PVA ( $M_w = 72,000$ ) were purchased from Sigma Aldrich (St. Louis, MO, USA). EUD L100 was procured from Ropharma (Milan, Italy). Methanol, sodium hydroxide, and hydrophosphoric acid were procured from Merck (Darmstadt, Germany). ERY was supplied from Dr. Reddy's Pharmaceutical Company, Bengaluru, India. Trypticase soy agar (TSA), thio-glycollate broth, soybean casein digest agar, and sabouraud dextrose agar were purchased from Merck (Seoul, South Korea). The bacterial strains *Micrococcus luteus* (ATCC 4698),

*Staphylococcus aureus* (ATCC 25923), and *Escherichia coli* (PTCC 1399) were procured from the American Type Culture Collection. All of the other compounds were of analytical grade and were used without further purification.

### 2.2. Preparation of ERY-Loaded Nanoparticles

EUD nanoparticles were prepared using the colloidal dispersion method and according to the method performed by Bodmeier et al., with some minor modifications [27]. Accordingly, specified amounts of EUD (10 mg/mL) and ERY (2 mg/mL) were dissolved in methanol and stirred (300 rpm) for 12 h at room temperature. The formed organic dispersion was then added dropwise to an aqueous solution of PVA in water (10 mg/mL), under magnetic stirring (800 rpm) until the nanoparticles were formed as a nanosuspension.

### 2.3. Preparation of Polymeric Ocular Inserts Containing ERY-Loaded Nanoparticles

Four different ocular inserts were prepared using CD- $\alpha$ , CD- $\beta$ , ALG, and GEL polymers according to a previous study [28]. A predetermined amount of each polymer was dissolved in the appropriate solvent, under magnetic stirring at 50 rpm to obtain a clear 1% *w/v* solution. A specified volume (1 mL) of each solution was added dropwise to the EUD/PVA nanosuspension. The resulting mixtures were poured into Petri dishes and dried in an oven at 60 °C for 18 h, producing nanoparticle-loaded ocular films. The prepared films were cut into small pieces of predetermined dimensions (inserts) and stored under sterile conditions for further investigations (Figure 1). The whole procedure took place under aseptic conditions.

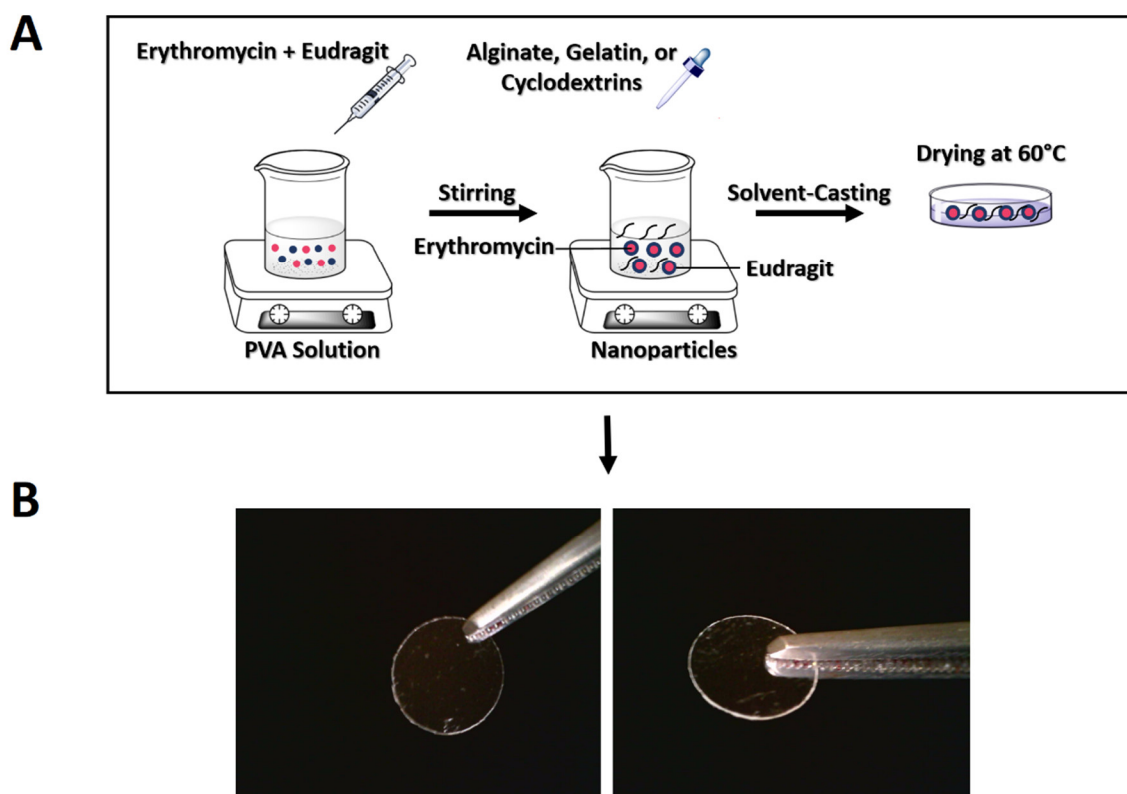


**Figure 1.** A schematic representation of the polymeric nanoparticle (PNP)-loaded film preparation procedure (**A**) visual appearance of nanoparticles-impregnated polymeric film insert (**B**).

### 2.4. Characterization of ERY-Loaded EUD/PVA Nanoparticles

#### 2.4.1. Lyophilization

The prepared drug-loaded nanoparticles were lyophilized using a freeze-drier (Christ Freeze Dryer ALPHA 2-4, PLUS, Osterode, Germany) after being ultracentrifuged (Beckman-

Coulter, Optima L-90K, Brea, CA, USA) at 30,000 rpm for 30 min at 4 °C [28]. Freezing took place at −85 °C for 4 h. The required time for vacuuming samples was 20 h at a negative pressure of 1.0 mbar.

#### 2.4.2. Size and Zeta Potential Analysis

The size distribution and Zeta potential of nanoparticles were determined by a Zeta-sizer (Nano-ZS, Malvern, UK). Five milligrams of lyophilized samples were dispersed in 5 mL of distilled water under continuous stirring at 300 rpm for 5 min at room temperature. After complete dispersion of the nanoparticles, a turbid suspension was obtained and introduced to the zeta-sizer [28].

#### 2.4.3. Entrapment Efficacy

To evaluate the entrapment efficiency (*EE*), the dispersion containing drug-loaded nanoparticles was centrifuged at 30,000 rpm for 20–30 min to separate nanoparticles from the supernatant containing a non-entrapped drug [28]. The amount of entrapped ERY was calculated by subtracting the amount of the non-entrapped ERY ( $W_{free\ ERY}$ ) that remained in the supernatant from the total amount of ERY used for the preparation of nanoparticles ( $W_{total\ ERY}$ ) divided by the total amount of drug ( $W_{total\ ERY}$ ) as formulated by Equation (1). The amount of non-entrapped drug in the supernatant was determined using a microbiological assay, which we explain in Section 2.9.

$$EE (\%) = \frac{W_{total\ ERY} - W_{free\ ERY}}{W_{total\ ERY}} \times 100 \quad (1)$$

#### 2.4.4. Drug Loading

The drug loading (*DL*) of nanoparticles was also determined according to the following equation, where  $W_{total\ ERY}$  stands for the total amount of ERY used for the preparation of nanoparticles,  $W_{free\ ERY}$  stands for the non-entrapped ERY, and  $W_{nanoparticles}$  stands for the total weight of lyophilized nanoparticles [28]. The amount of non-entrapped drug in the supernatant was determined using the microbiological assay.

$$DL (\%) = \frac{W_{total\ ERY} - W_{free\ ERY}}{W_{nanoparticles}} \times 100 \quad (2)$$

### 2.5. Characterization of Ocular Inserts Containing ERY-Loaded Nanoparticles

#### 2.5.1. Thickness

The thickness uniformity is an important factor that should be considered in the evaluation of ocular inserts. The thickness was determined at six different points of each polymeric insert using a digital micrometer (Tork Craft Digital Micrometer, 0–25 mm, ME30025, Quanzhou, China) and the average was taken.

#### 2.5.2. Folding Endurance

The prepared inserts were folded at the center repeatedly until they break or crack. The number of folding an insert could resist without breaking (folding endurance) was recorded. The test was repeated in triplicate and an average was taken. Folding endurance is a key factor in the determination of film flexibility [29].

#### 2.5.3. Percentage of Swelling

The swelling percentage of each ocular insert was determined by soaking them in a phosphate buffer (pH 7.4) at 37 °C. At the predetermined time intervals (30, 60, 90, and 120 min) inserts were weighed after the elimination of surface water using a filter paper, and based on the weight change through different times the swelling was calculated using

Equation (3), where  $W_t$  stands for the measured weight at time  $t$  and  $W_0$  is the initial weight of inserts [29]:

$$\text{Swelling (\%)} = \frac{W_t - W_0}{W_0} \times 100 \quad (3)$$

#### 2.5.4. Moisture Loss and Moisture Uptake

The moisture loss and uptake of ocular inserts were determined to ensure their stability and uniformity under dry and humid conditions [29]. These tests were carried out by putting a pre-weighed piece of polymeric film in a desiccator containing anhydrous calcium chloride (dry condition) and a saturated solution of aluminum chloride (humid condition) for three days. The final weight of each sample was then recorded and the percentages of moisture loss and uptake were determined by the formula described in Equation (4). The  $W_f$  and  $W_0$  denote the final weight and the initial weight of the inserts, respectively.

$$\text{Moisture loss and uptake (\%)} = \frac{|W_f - W_0|}{W_0} \times 100 \quad (4)$$

#### 2.5.5. Surface pH

The surface pH of inserts was measured by placing each insert in a Petri dish containing 2% *w/v* agar in phosphate buffer (pH = 7.4) for 5 h under stirring conditions. The surface pH was measured using a pH meter (827 pH lab, Metrohm, Herisau, Switzerland). A mean of three readings was calculated.

#### 2.5.6. Tensile Strength

The tensile strength of the obtained inserts was studied using a universal mechanical testing machine (STM50, Santam, Tehran, Iran) [28]. Polymeric films with dimensions of 30 × 15 mm and a thickness of 1 mm were placed into the clamps and the stretching force was applied to samples to obtain tensile strength. Upon breaking, the amount of applied force and the elongation of films at break were recorded.

#### 2.5.7. Ex Vivo Mucoadhesion Time

A method adopted by Tofighia et al. [30] with slight modifications was utilized to determine the mucoadhesion time of formulations. There are also other similar methods to determine the mucoadhesive time [31,32]. Freshly excised sheep cornea was obtained from a slaughterhouse and attached by a two-sided glue tape to a microscope slide. The slide was fixed to the basket of a disintegration apparatus filled with 900 mL PBS (pH = 7.4). The inserts were brought into contact with and pressed for 15 s onto the excised sheep cornea (hydrated with PBS). The disintegration apparatus was run where the fixed microscope slides moved upward and downward to come out and soak in the PBS repeatedly at a constant rate. The temperature was kept at 37 °C. The time required for the mounted inserts to completely detach from the cornea was recorded as the mucoadhesion time. The test was repeated three times for each sample.

#### 2.6. Fourier Transform Infrared Spectroscopy (FTIR)

The FTIR analysis was performed to evaluate the drug-polymer compatibility and to detect any alteration of drug structure during preparation. FTIR spectra of ERY, PVA, EUD, drug-loaded ocular inserts and all polymers used for the preparation of inserts were generated by an FTIR spectrophotometer (IRprestige-21, Shimadzu Co., Tokyo, Japan) using the potassium bromide (KBr, 99.99%, Sigma-Aldrich, Burlington, MA, USA) pellets method [33]. The samples were ground with KBr and then were compressed into analytical pellets using a manual press under 10 tons pressure for 10 min. The spectra were recorded between 4000 to 400  $\text{cm}^{-1}$ .

### 2.7. Scanning Electron Microscopy (SEM)

The morphology of drug-loaded nanoparticles on the surface of polymeric films was observed by a scanning electron microscope (SEM TESCAN, MIRA3, Brno, Czech Republic). Samples were placed on the aluminum stub and were gold-coated prior to SEM imaging [33]. The accelerating voltage was set at 20 kV.

### 2.8. Antibacterial Efficacy

The inhibitory effect of prepared inserts on gram-positive and gram-negative bacteria was studied using *Staphylococcus aureus* (*S. aureus*) and *Escherichia coli* (*E. coli*), respectively, by the disk diffusion method [28]. Bacterial strains were cultured in tryptic soy broth (TBS) and incubated at 35 °C for 24 h, then diluted. Drug-loaded ocular inserts were cut into round disks of 6 mm diameter and placed onto TSA plates inoculated with bacterial suspensions, then incubated at 35 °C for 24 h. The zones of growth inhibition were observed and determined to evaluate the inhibitory effect of inserts.

### 2.9. Microbiological Assay

According to previous reports, ultraviolet (UV) spectroscopy or high-performance liquid chromatography (HPLC)-UV methods are not suitable for the quantification of pure ERY [34–36]. Complicated derivatization is required in the case of drugs with weak UV absorption [37]. Also, according to USP, ERY assay is mainly performed by microbial assay, which has comparable accuracy to the HPLC method [34,35]. Therefore, this method was utilized in the present study. This method also has the advantage of a low limit of detection (LOD) [38]. As the disk diffusion method is used to perform the microbial assay, where a flexible disk is soaked with tear samples, there is therefore no need for invasive methods such as surgery, animal euthanasia or the sacrificing of animals [39,40].

The calibration curve of  $\log_{10}$  of ERY concentration versus the diameter of the inhibition zone was constructed by microbiological assay [28]. A specific amount of ERY standard solutions in methanol (250, 125, 62.5, 31.25, 15.62, 7.81, and 3.90  $\mu\text{g}/\text{mL}$ ) was separately added to sterile blank disks and followed by drying the samples at room temperature. A McFarland standard suspension of *Micrococcus luteus* (*M. luteus*) was uniformly spread onto the TSA plates, then the disks were placed on the plates and incubated for 24 h at 35 °C. The diameter of inhibition zones was measured using a micrometer. All of the experiments were repeated three times and the mean  $\pm$  SD at different concentrations were plotted to generate the calibration curve. The inter-day and intra-day accuracy of this method was determined and used as validation parameters.

### 2.10. In Vitro Release Study

To evaluate the release characteristics of ERY, a bi-chambered donor–receptor compartment model was assembled [28]. ERY ophthalmic ointment (Erythrolidine<sup>®</sup>, Sina Darou, Tehran, Iran), CD- $\alpha$ , CD- $\beta$ , GEL, and ALG film inserts were subjected to in vitro release study. Eighty milligrams of each film insert formulation and 0.2 mg of ointment (along with 1 mL of PBS) were placed in a donor chamber that was separated from the receptor chamber (containing 24 mL PBS at pH of 7.4) using a dialysis membrane (Mw cutoff = 12,000–14,000 Daltons; Delchimica Scientific Glassware, Milan, Italy). At specific time intervals (1, 3, 5, 9, 14, 26, 38, 50, 74, 146 h), 100  $\mu\text{L}$  samples were withdrawn and the whole receptor medium was replaced with fresh buffer (kept at the same temperature). The concentration of drugs retrieved from the receptor compartment at different time points was determined using the regression equation obtained by the microbiological assay method (described in Section 2.9). All the release experiments were repeated three times.

The release data were fitted to different kinetical models to predict the mechanism of drug release from inserts. The model with the highest correlation coefficient ( $R^2$ ) was selected as the best-fitted model.

### 2.11. Sterility Test

In order to maintain sterility, all ocular inserts were prepared under aseptic conditions. All of the prepared ocular inserts were exposed to UV light for 15 min and then were subjected to the sterility test. The sterility test was performed as per the USP guidelines. For this purpose, samples were placed for 28 days in three different culture media: (a) sodium thioglycolate broth to detect the growth of any anaerobic bacteria, (b) soybean-casein digest broth to observe aerobic bacterial contamination, and (c) sabouraud dextrose broth for determination of fungal growth. Positive and negative controls were used.

### 2.12. In Vivo Ocular Irritation

The Draize ocular irritation test was carried out on four male New Zealand albino rabbits, weighing 3.5–4 kg according to the method utilized by Gagandeep et al. [41]. Each of the prepared inserts along with 100  $\mu$ L sterile PBS was separately placed in the cul-de-sac of the right eyes of a rabbit. An equal volume of phosphate buffer was used as a control in the left eyes of rabbits. The symptoms of ocular irritation or damage to the cornea, iris, and conjunctivae including abnormal discharge, conjunctival redness, swelling, corneal opacity, etc. were observed and scored on a 3-grade scale (0 = no alteration, 1 = mild alteration, 3 = obvious alteration) [42]. The sum of the scores obtained for each category was calculated.

### 2.13. In Vivo Bioavailability Study

The in vivo release of ERY from ocular inserts was determined using male New Zealand albino rabbits weighing 3.5 to 4 kg [28]. The animals were kept under the same diet and conditions. Before the test, the eyes of rabbits ( $n = 30$ ) were washed with phosphate buffer. Small circular pieces ( $\varnothing = 5$ –6 mm) of ocular inserts (25 mg) containing 1.265 mg of ERY with 100  $\mu$ L buffer were inserted in the conjunctival sac of animals. The marketed ophthalmic ointment of ERY (Erythrolidine<sup>®</sup>, Sina Darou, Tehran, Iran) was also examined as a control. At specific time intervals, samples were taken from the tears of rabbits by a novel, non-invasive method without the requirement for any surgical intervention which can cause discomfort to animals. Briefly, sterile paper discs with a diameter of 5 mm were soaked for 10 s with tear samples of rabbits and then assayed with the microbiological disk diffusion method described in Section 2.9.

### 2.14. Statistical Analysis

In the present study, all the experiments were carried out in triplicate, and data were reported as mean  $\pm$  SD. Statistical analyses were carried out using the paired T-test and Kruskal-Wallis tests. The statistical significance for all tests was confirmed at  $p < 0.05$ .

## 3. Results and Discussion

### 3.1. Characterization of ERY-Loaded EUD/PVA Nanoparticles

Colloidal dispersion methods are commonly used for producing nanoparticles aiming at high entrapment efficiency, stability, and low toxicity. In the present study, a nanoparticle formulation was prepared for ocular delivery of ERY, using EUD as a coating polymer in the presence of PVA as a dispersing agent. Different formulations were prepared by changing experimental variables including the concentration of polymers, concentration of polyvinyl alcohol as a dispersant agent, and the weight ratio of drug to polymers, and the best set of these variables was chosen as the optimized formulation. Accordingly, the optimized formulation was developed resulting from a solution of EUD (10 mg/mL) and ERY (2 mg/mL) at a PVA concentration of 10 mg/mL. The higher concentrations of polymers led to larger particle sizes and higher viscosity which can avoid the formation of smaller particles by increasing the surface tension [43]. The mean particle size obtained for the formulation was in an appropriate nano-range ( $66.44 \pm 4.19$  nm), and the size distribution was narrow enough ( $PDI = 0.40 \pm 0.03$ ), to have a uniform distribution. This small particle size has the advantage of the increased surface-to-volume ratio resulting in enhanced solubility and bioavailability of the drug. Furthermore, formulations with

nano-range particle sizes are less likely to cause any irritation to the eye [4]. In addition, nanoparticles showed a negatively charged Zeta potential ( $-6.03 \pm 2.34$  mV), which could mainly be attributed to the negative charge of EUD [44]. To achieve a suitable *EE*%, an optimized viscosity of PVA solution should be preserved (10–20 mPa.s) to prevent solubilizing of the drug in the aqueous phase. The *EE*% of nanoparticle formulation was up to  $50.71 \pm 3.16\%$ , showing promising entrapment of ERY in the nanoparticles [45] (Table 1).

**Table 1.** Particle characteristics, drug entrapment, and loading of developed nanoparticle formulation.

Formulation	Particle Size (nm)	Polydispersity Index	Zeta Potential (mV)	DL (%)	EE (%)
Nanoparticles	$66.44 \pm 4.19$	$0.40 \pm 0.03$	$-6.03 \pm 2.34$	$22.41 \pm 2.55$	$50.71 \pm 3.16$

Abbreviations: DL (Drug Loading), EE (Entrapment Efficiency).

### 3.2. Characterization of Ocular Inserts

Nanoparticles were incorporated into different polymeric films to form inserts suitable for the ocular delivery of ERY. Ocular inserts were produced from different polymers by the solvent-casting method [46]. All of the prepared polymeric films had uniform and homogenous surfaces and were sufficiently transparent with no visible cracks or imperfections, corroborating the efficiency of the method used for the preparation of inserts. An ALG-based ocular insert is shown in Figure 1B.

The measured weight variation and thickness of different polymeric films are shown in Table 2. Accordingly, the GEL formulation was the heaviest, followed by CD- $\alpha$  films. ALG films were the lightest of all the prepared inserts. The sufficient thickness uniformity of all prepared films is another finding which can be concluded from the obtained data. The thinnest film was found to be that of ALG ( $0.148 \pm 0.004$  mm), while the greatest thickness belonged to GEL ( $0.172 \pm 0.002$  mm). The low standard deviation for different formulations indicates the acceptable uniformity of all prepared polymeric films.

**Table 2.** The physicochemical-mechanical characteristic of developed inserts.

Parameter	Formulations			
	ALG	GEL	CD- $\alpha$	CD- $\beta$
Weight (mg)	$20.19 \pm 0.65$	$23.61 \pm 0.25$	$22.14 \pm 0.20$	$21.63 \pm 0.30$
Thickness (mm)	$0.148 \pm 0.004$	$0.172 \pm 0.002$	$0.170 \pm 0.006$	$0.155 \pm 0.003$
Folding endurance (times)	$227.0 \pm 5.2$	$355.3 \pm 6.1$	$341.0 \pm 8.5$	$303.1 \pm 8.1$
pH	$6.64 \pm 0.03$	$6.69 \pm 0.02$	$6.50 \pm 0.02$	$6.52 \pm 0.04$
Tensile Strength (MPa)	$2.10 \pm 0.01$	$3.42 \pm 0.01$	$2.35 \pm 0.07$	$2.30 \pm 0.01$
Swelling (%)	30 min	$55.3 \pm 0.8$	$101.0 \pm 1.9$	$74.3 \pm 0.4$
	60 min	$91.2 \pm 0.8$	$189.0 \pm 3.6$	$154.0 \pm 3.6$
	120 min	$147.3 \pm 0.8$	$194.0 \pm 1.9$	$174.3 \pm 1.9$
Moisture uptake (%)	$0.77 \pm 0.07$	$2.08 \pm 0.09$	$1.62 \pm 0.08$	$0.88 \pm 0.13$
Moisture loss (%)	$1.16 \pm 0.05$	$1.60 \pm 0.07$	$0.51 \pm 0.08$	$0.97 \pm 0.13$
Mucoadhesion time (min)	$8.4 \pm 0.4$	$9.2 \pm 0.2$	$9.4 \pm 0.3$	$10.7 \pm 0.5$

The folding endurance was another important property examined in this study. This parameter indicates the ability of each film to withstand frequent folding, which is important for the production, shipping, and handling of the insert. According to the results, all the prepared films possessed appropriate folding endurance withstanding 227–355 folds (Table 2). As shown in Table 2, GEL was the most resistant/durable, starting to crack but not break after 355 times of folding. The results of folding endurance confirm the desirable film-forming capability of the processed polymers, especially gelatin, and indicates that these inserts can potentially be used as inserts with sufficient mechanical flexibility [47,48].

The weight variation for each polymeric film, due to swelling, during the 2 h study is presented in Table 2. The results indicate that throughout the study period, the swelling percentage of the drug-loaded GEL insert was greater than other formulations with an



almost 200% increase in weight. This could be attributed to the higher hydrophilicity of GEL, thus a high capacity to absorb water by the polymer network. The swelling percentage is likely to affect drug release from the formulations. The least swelling percentage was demonstrated by ALG (less than 150%).

It was observed that uptake and loss of moisture were insignificant in all the formulations (all less than 3%). ALG and GEL films were found to gain the least and the highest amount of moisture, respectively. The highest and lowest percentage of moisture loss was attributed to the GEL insert and CD- $\alpha$  insert, respectively. These results indicate that polymeric films have an acceptable hindrance to moisture transfer and are likely to be stable in both dry and wet conditions [49].

Surface pH is one parameter that should be evaluated as part of the development of any topical ophthalmic products as it is likely to affect their biocompatibility. Generally, topical ophthalmic formulations may cause discomfort, and irritation and induce reflex tear production leading to faster drug elimination via nasolacrimal drainage. In this study, all the formulations possessed a pH (between 6.5 and 6.7) which can be well tolerated by the eyes and cause minimal irritation and discomfort [50,51].

The formulations were ranked from highest to lowest tensile strength as follows: GEL > CD- $\alpha$  > CD- $\beta$  > ALG. The tensile strength of all the formulations was in the range of  $2.10 \pm 0.01$  to  $3.42 \pm 0.01$  MPa, corresponding to ALG and GEL films, respectively. In a similar study, the tensile strength of 1.7 MPa was considered suitable for ocular administration [52]. Furthermore, multiple studies reported tensile strength values in a range of 1–3 MPa for similar ocular inserts [53,54]. The importance of having a suitable tensile strength is that the ocular insert would resist fast erosion (pulse drug release and rapid elimination) as well as showing little or no discomfort as a result of eye movements [55].

The investigated formulations showed a mucoadhesion time of between 8.4 to 10.7 min that is significantly enhanced compared to conventional eye formulations that are eliminated from the eye immediately (within 60–90 s) after administration. Table 2 presents the mucoadhesion times for different formulations to the sheep cornea. The CD- $\alpha$  and CD- $\beta$  inserts provided the longest mucoadhesion times due to their hydrophilic nature. GEL also showed prolonged mucoadhesion time to the cornea compared with ALG, which could be ascribed to the relatively higher hydrophobicity of ALG. It is anticipated that the developed formulations would show longer residence times in vivo.

### 3.3. Fourier Transform Infrared Spectroscopy (FTIR)

Figure 2 outlines the FTIR spectra of ERY, the polymers, and the ocular inserts. All formulations retain the characteristic peaks of ERY. The peak appeared around  $3464 \text{ cm}^{-1}$  and is assigned to the OH group of ERY. Peaks at around  $1732$  and  $1685 \text{ cm}^{-1}$  are attributed to ketone and lactone groups of ERY, respectively.  $\text{CH}_2$  bending of ERY also appeared between  $1340$ – $1460 \text{ cm}^{-1}$ . The characteristic peaks of EUD appeared around  $1728$  and  $1388 \text{ cm}^{-1}$ , respectively corresponding to  $\text{C}=\text{O}$  vibration and  $\text{CH}_2$  stretching. Peaks at around  $2800$ – $2900 \text{ cm}^{-1}$  representing the symmetrical and asymmetrical  $\text{CH}_2$  bond stretching are attributed to PVA, EUD, and matrices' polymers. Peaks appeared at  $1000$ – $1100 \text{ cm}^{-1}$ , assigned to the C-O and C-O-C bond stretching of polymers. The FTIR spectrum obtained for each formulation represents the characteristic peaks of the polymers used in the preparation of the formulation along with the characteristic peaks of the drug. Based on the obtained results, it can be concluded that there was no interaction between the drug and the polymers and there is polymer-drug compatibility. It seems that a polymer-polymer interaction has occurred between the methacrylic acid functional group of EUD and GEL according to the obtained spectrum of GEL insert [56]. The appearance of new peaks in GEL inserts spectrum in the range of  $1600$ – $3400 \text{ cm}^{-1}$  which is due to N-H stretching confirming the engagement of GEL amine groups in the abovementioned interaction.

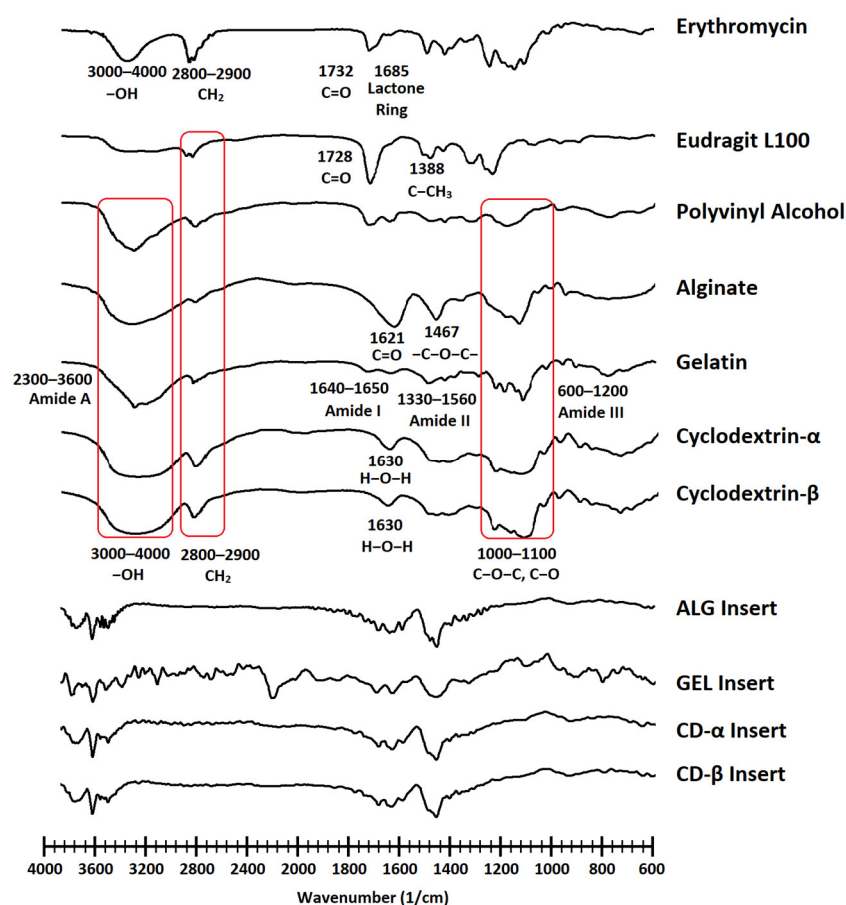


**Figure 2.** The FTIR spectra of erythromycin, polymers, and ocular inserts (ALG, GEL, CD- $\alpha$ , and CD- $\beta$  inserts).

### 3.4. Scanning Electron Microscopy (SEM)

Scanning electron micrographs revealed almost multi-dimensional, drug-loaded nanoparticles without aggregation (Figure 3). The nanoparticles possessed a smooth and uniform surface. As was previously reported, the loading of nanoparticles on the surface of polymeric films instead of distributing through the polymeric matrix could cause surface roughness [57]. The SEM photograph of polymeric films loaded with nanoparticles illustrates the uniform distribution of the nanoparticles in the polymeric matrices of the fabricated films. The uniform distribution of nanoparticles in the polymeric matrix of inserts was observed for all prepared formulations (Figure 3).

### 3.5. Antibacterial Efficacy

Figure 4 represents the antibacterial efficacy of ocular inserts against *S. aureus* and *E. coli*. The mean diameter of the inhibition zone in the presence of each prepared insert was determined and compared. At first glance, the inhibition zone could be observed in the vicinity of all the drug-loaded inserts against both gram-positive and gram-negative bacterial strains (Figure 4). Based on the previous reports, ERY has an antibacterial efficacy against both gram-positive and gram-negative bacteria [58,59]. From Figure 4, it is obvious that the antibacterial efficacy of ERY was preserved in the ocular inserts. However, no inhibitory activity could be observed in the plates containing blank inserts. The diameter of the inhibition zone was found to be larger in the presence of *E. coli*, in comparison with *S. aureus*, indicating the better antibacterial potential of ocular inserts against gram-negative bacteria.

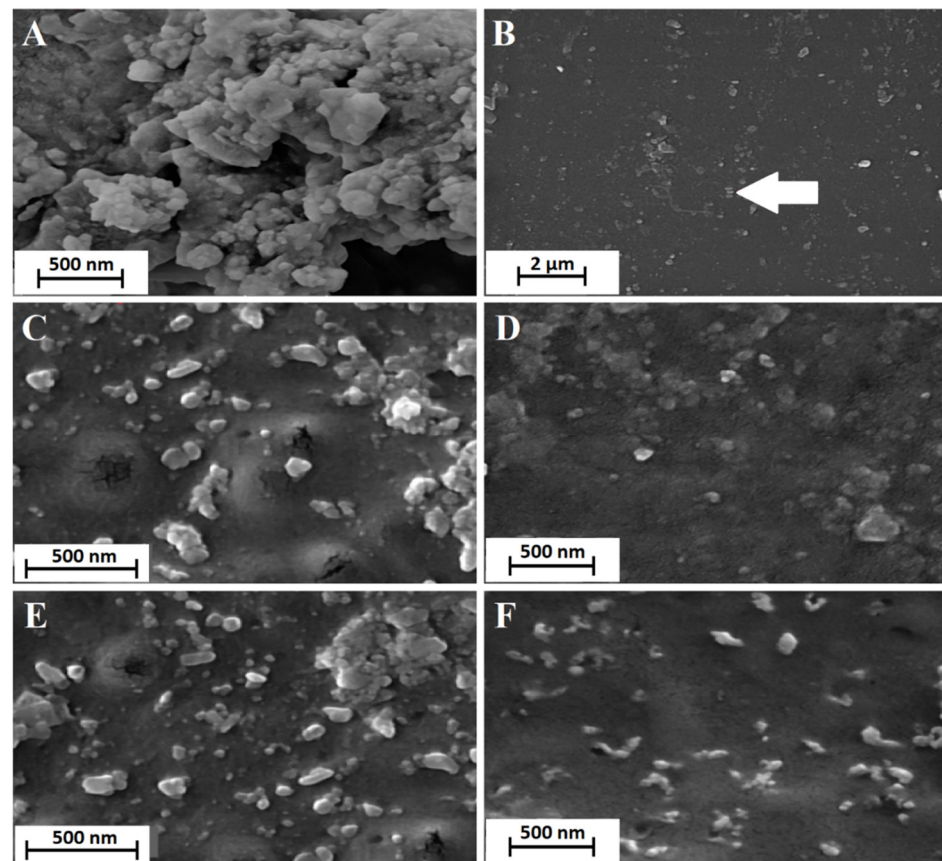


**Figure 3.** SEM images of erythromycin-loaded nanoparticles (A,B), CD-β insert (C), GEL insert (D), ALG insert (E), and CD-α insert (F).

### 3.6. Microbiological Assay

The microbiological assay against *M. luteus* was carried out to construct the calibration curve of ERY in the concentration range of 3.90–250.00 μg/mL. The calibration curve followed the regression equation of  $1.2528x + 0.0229$  ( $R^2 = 0.9690$ ); where Y is the mean diameter of the zone of inhibition and X is the concentration of ERY. The inter-day and intra-day accuracy and precision of the method were evaluated at three different concentrations of the drug (Table 3). The results corroborated the acceptable accuracy and precision of the method for the determination of drug concentration through the study.

**Table 3.** The intra- and inter-day accuracy and precision for the microbial assay method measuring three different inhibitory concentrations of erythromycin against *M. luteus*.

Concentration of ERY (μg/mL)	Accuracy (%)		Precision (CV %)	
	Intra-Day	Inter-Day	Intra-Day	Inter-Day
125	102.947	112.268	0.494	0.703
62.5	94.581	114.266	0.401	0.477
31.25	116.908	110.410	0.418	0.520

Abbreviations: ERY (Erythromycin), CV (coefficient of variation).

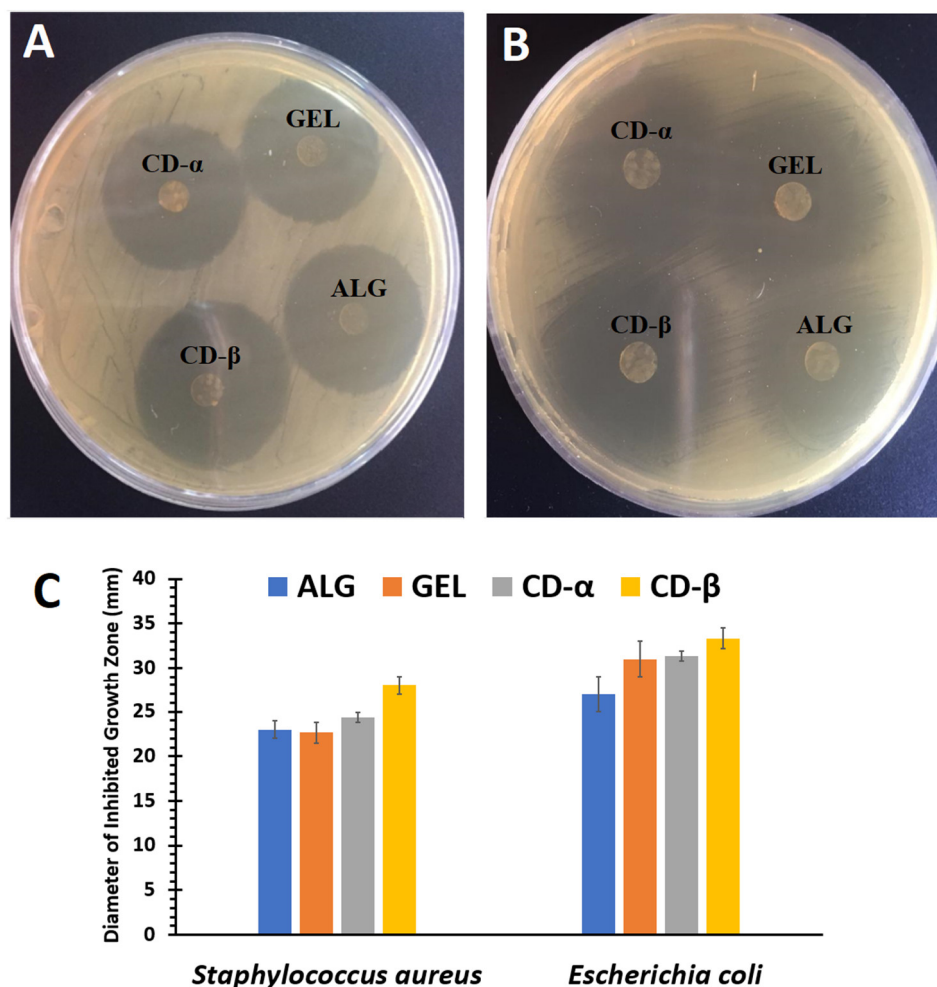


**Figure 4.** The antibacterial efficacy of ERY-loaded GEL, ALG, CD- $\alpha$ , and CD- $\beta$  ocular inserts against *E. coli* (A) and *S. aureus* (B), and the comparative graph (C) of the diameter of inhibited growth zones (mm) obtained for inserts against these microorganisms ( $n = 3$ ).

### 3.7. In Vitro Release Study

The in vitro release profile of ERY from EUD/PVA nanoparticles, loaded in different ocular inserts along with the nanosuspension, is illustrated in Figure 5. The most striking feature of the developed formulations was the sustained release pattern of the drug over more than 140 h compared to the ointment formulation, which released more than 90% of its drug content during the first 5 h. It seems that despite the hydrophobic nature of the base of this ointment, which is white petrolatum, the formulation was not able to release the drug in a controlled manner. The reason behind this rapid release is that the drug is suspended and not dissolved in the ointment base as it is highly water-soluble; hence, right after placement in the test apparatus at the temperature of 37 °C, the ointment base melted and the drug was rapidly released into the receptor medium. All the insert formulations potentially released 40–80% of their drug content over a prolonged duration (Figure 5). Through the first 12 h, all insert formulations released between approximately 15–35% of their drug content which was followed by a slow-release phase. From the release profiles presented in Figure 5, it can be seen that amongst the investigated inserts, CD- $\alpha$ , CD- $\beta$ , and ALG showed the most promising release profile by releasing  $82.76 \pm 3.22\%$ ,  $59.85 \pm 1.75\%$ , and  $48.69 \pm 1.12\%$  of the drug in 146 h.

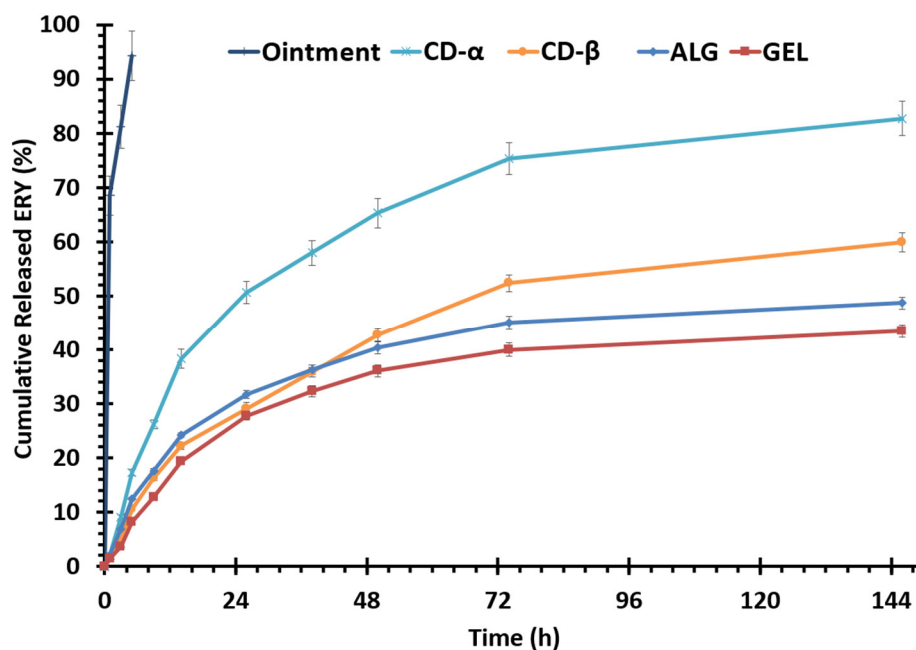


**Figure 5.** Cumulative release of erythromycin (expressed as a percentage) vs time profiles for the marketed ophthalmic ointment of erythromycin, GEL, ALG, CD- $\alpha$ , and CD- $\beta$  ocular inserts in PBS (pH = 7.4) at 37 °C.

The release profile clearly shows a controlled release process of ERY. The steeper slope of the release profile during the initial hours of the study has likely occurred due to the fast release of the drug loaded onto or near the surface of nanoparticles, which is followed by a sustained-release of the ERY distributed in the polymeric matrix. The CD- $\alpha$  and CD- $\beta$  ocular inserts showed higher percentages of the released drug due to the higher water solubility of matrix polymers and higher swelling percentage compared to the ALG insert [60]. Despite the higher degree of swelling compared to ALG, GEL indicated the lowest amount of released drug probably due to the interaction that occurred between GEL and EUD that led to a semi-rigid structure that inhibits the drug release [56]. A similar result was reported by Cetin et al., who designed and evaluated the diclofenac sodium-loaded EUD nanoparticles [44]. A 55-day release of the antifungal drug itraconazole was reported in a similar study [29].

Table 4 represents the R<sup>2</sup> values obtained by fitting release data to different kinetical models. All formulations followed the Higuchi kinetical model. This indicated that the formulations released the drug mainly by the diffusion phenomenon. Accordingly, during the initial hours, the surface-loaded drug was released at a more rapid rate; the dissolution medium was then diffused into the inserts and dissolved the drug at a sustained rate.

**Table 4.** The correlation coefficients obtained by fitting the release data in different kinetical models.

Formulation	Correlation Coefficient (R <sup>2</sup> )			
	Zero-Order	First-Order	Higuchi	Korsmeyer-Peppas
ALG	0.9030	0.9341	0.9847	0.9606
GEL	0.9400	0.9595	0.9898	0.9572
CD- $\alpha$	0.9096	0.9614	0.9858	0.9465
CD- $\beta$	0.9325	0.9579	0.9839	0.9837

### 3.8. Sterility Test

After sterilization of ocular inserts by UV irradiation, the growth of microorganisms in the presence of each ocular film containing blank nanoparticles was examined. Different

groups including a positive control, negative control, and test groups were visually examined. No significant change was observed in the turbidity of media for the negative control and test tubes, while in the positive control the growth of microorganisms was detected. According to these results, it can be concluded that the whole procedure was aseptic, the ocular inserts were sterile, and that they could be confidently used for in vivo study.

### 3.9. Irritation Test

The possibility of inducing irritation after the insertion of ocular inserts in the eyes of the rabbit was examined by the Draize test to ensure that the prepared inserts can be potentially used by humans without causing pain or discomfort. Upon placing ocular inserts in the eyes of rabbits, at specific time intervals (0 h, 24 h, 48 h, and 72 h) the eyes were carefully inspected. The obtained scores are classified in Table 5. Also, Figure 6 indicates the result of the irritation test for one of the ocular inserts and control groups. Irritancy scores of GEL, CD- $\alpha$ , and CD- $\beta$  were observed to be 0 within three days. There was no sign of irritation, redness, swelling, corneal opacity, intensive tearing, frequent blinking, or any other visible abnormality for any of the formulations except for ALG, which showed a mild redness during the first day of administration. The appearance was similar to control eyes. As for the fact that rabbits possess eyes that are more vulnerable to damage and irritation than humans, it could be generalized that such formulations can be inserted into human eyes without causing any significant irritation or abnormalities [61].

**Table 5.** Ocular irritation test according to Draize test.

Formulation	Time (h)	Cornea		Iris	Conjunctivae			Total Score
		Opacity	Area of Cornea Involved	Interruption for Reaction to Light	Redness	Chemosis	Discharge	
Control	24	0	0	0	0	0	0	0
	48	0	0	0	0	0	0	0
	72	0	0	0	0	0	0	0
ALG	24	0	0	0	1	0	0	1
	48	0	0	0	0	0	0	0
	72	0	0	0	0	0	0	0
GEL	24	0	0	0	0	0	0	0
	48	0	0	0	0	0	0	0
	72	0	0	0	0	0	0	0
CD- $\alpha$	24	0	0	0	0	0	0	0
	48	0	0	0	0	0	0	0
	72	0	0	0	0	0	0	0
CD- $\beta$	24	0	0	0	0	0	0	0
	48	0	0	0	0	0	0	0
	72	0	0	0	0	0	0	0

### 3.10. In Vivo Tear Fluid Bioavailability Study

Taking the in vitro release results into consideration, all formulations (CD- $\alpha$ , CD- $\beta$ , GEL, and ALG) have been subjected to in vivo study. In this study, sampling from the animal tears was done by a novel method that is more animal-friendly and has been set up for the first time by our team in a previous study [28], hence a possible alternative to using common invasive sampling methods. In previous investigations, in vivo sampling required anesthetizing or sacrificing animals [62]; however, in this study sampling was performed by collecting the rabbits' tears using a sterile paper disk which was then assayed by the microbial assay for ERY content. To the best of our knowledge, no previous studies have reported on a similar method of in vivo sampling.

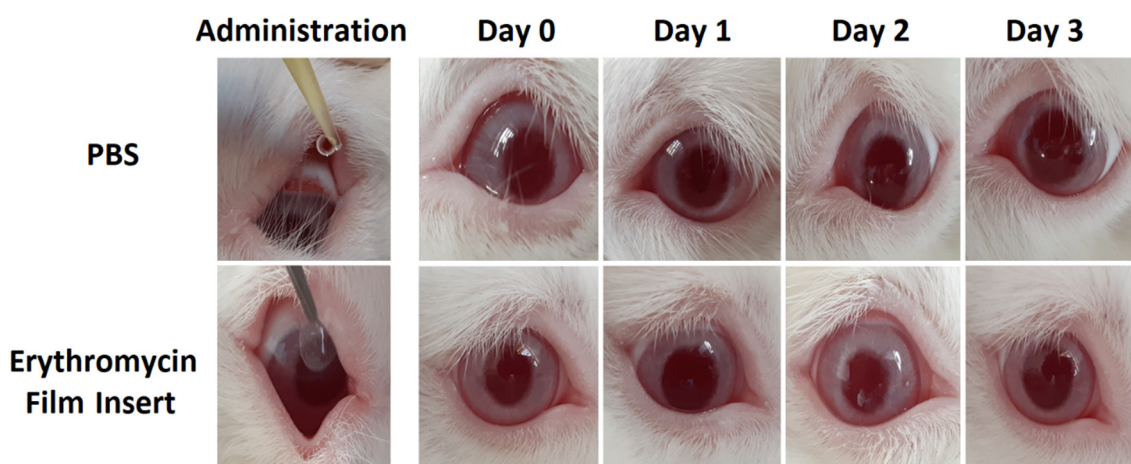


**Figure 6.** Images of rabbits' eyes treated with phosphate buffer solution (PBS) and ALG ocular insert during 3 days of examination by Draize test.

According to Figure 7, a sharp peak appeared in the tear fluid release profile of ERY described as  $C_{max}$  for all formulations at the initial hours reaching  $2990.35 \pm 133.20$ ,  $2945.43 \pm 196.72$ ,  $1845.21 \pm 286.60$ , and  $2640.18 \pm 234.97$   $\mu\text{g}/\text{mL}$  for GEL, ALG, CD- $\alpha$ , and CD- $\beta$  inserts, respectively. Meanwhile, the marketed formulation could reach a  $C_{max}$  of  $1309.91 \pm 260.90$   $\mu\text{g}/\text{mL}$ , which is significantly lower than the film inserts. The sharp peak indicates the burst release of ERY from each formulation, which could be considered beneficial. This high amount of released drug can cause an initial shock against microorganisms. As has been proven in previous studies, topical formulations have the drawback of poor absorption and precorneal loss, which leads to the fact that only about 1–10% of the drug can be absorbed intraocularly [63]. The developed inserts can beneficially prolong the residence time of the drug on the ocular surface four times longer than the marketed formulation. The ophthalmic ointment was washed out of the conjunctival sac within 5 h of investigation, and after this interval, the drug was not detectable in the tear fluid. Also, as mentioned earlier, due to high water solubility, ERY is not soluble in the ointment base and is washed out of the eye right after administration and the dissolving of the ointment in the conjunctival sac.

Increasing the ocular-surface (tear fluid) availability of ERY is likely to increase the intervals needed between drug administrations, thus overcoming the requirement for frequent use of the drug where fewer side effects are expected. This is likely to improve patient compliance due to less frequent administration. Another positive aspect of the studied formulations is that the tear concentration of ERY is beyond the MIC against microorganisms over 120 h of in vivo analysis. The most  $AUC_{0-120}$  was measured for CD- $\beta$ , followed by GEL, CD- $\alpha$ , and ALG, respectively. The pharmacokinetic parameters of the developed insert are indexed in Table 6.

**Table 6.** The pharmacokinetic parameters of ERY-loaded ocular inserts tested in the rabbits' eyes ( $n = 30$ ).

Formulation	$C_{Max}$ ( $\mu\text{g}/\text{mL}$ )	$AUC_{0-120}$ ( $\mu\text{g}\cdot\text{h}/\text{mL}$ )	MRT (h)
Ointment	$1309.91 \pm 260.90$	$4986.62 \pm 630.85$	$3.67 \pm 0.16$
ALG	$2945.43 \pm 196.72$	$30,020.92 \pm 45.54$	$24.85 \pm 0.01$
GEL	$2990.35 \pm 133.20$	$33,917.77 \pm 3023.76$	$21.91 \pm 0.10$
CD- $\alpha$	$1845.21 \pm 286.60$	$32,786.23 \pm 3550.15$	$21.60 \pm 0.48$
CD- $\beta$	$2640.18 \pm 234.97$	$35,938.29 \pm 602.54$	$28.27 \pm 0.14$

Abbreviations:  $C_{Max}$  (Maximum Concentration), AUC (Area Under the Curve), MRT (Mean Residence Time).

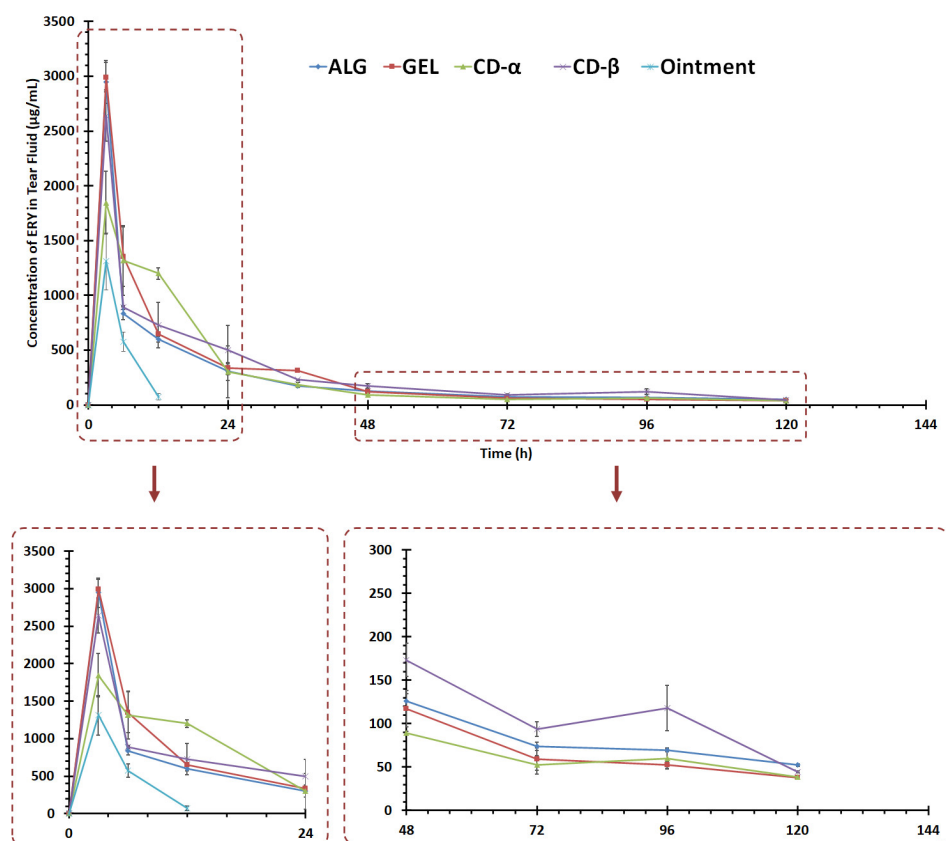


**Figure 7.** ERY concentration in tear fluid following administration of marketed ophthalmic ointment of erythromycin, ALG, GEL, CD- $\alpha$ , and CD- $\beta$  ocular inserts ( $n = 30$ ).

In a similar investigation, a nanoparticles impregnated ocular insert containing acetazolamide was prepared. The data obtained from in vivo studies indicated an enhanced therapeutic effect of nanoparticle formulation compared to a conventional solution [57]. As reported by Chhonker et al., amphotericin B-loaded nanoparticles showed an enhanced pharmacokinetic effect compared to the marketed formulation [64]. Taghe et al. have reported the same sustained-release profile of azithromycin for ocular administration from mucoadhesive films impregnated with nanoparticles [28]. In a similar study, EUD-based nanofibrous inserts indicated the sustained release of ofloxacin with a tear concentration above the MIC for 96 h [65].

#### 4. Conclusions

Four different mucoadhesive polymeric film formulations containing ERY-loaded EUD/PVA nanoparticles were designed and developed as ocular inserts to overcome the challenges related to the administration of conventional eye formulations including limited bioavailability, short residence time, and the requirement of frequent administration. The developed nanoparticles possessed suitable particle size and over 50% entrapment efficacy. All ocular inserts indicated strength, flexibility, and proper mechanical properties to be used on the ocular surface without undesirable effects. No interaction between drug and polymers was observed and morphological examination indicated a uniform surface with a good distribution of nanoparticles in the polymeric matrices. All formulations showed antimicrobial efficacy against *E. coli* and *S. aureus*. The in vitro study showed a controlled release profile extending over six days. CD- $\alpha$  and CD- $\beta$  inserts showed the most promising in vitro release profiles by releasing 60–80% of the drug in 144 h. A novel non-invasive technique was established for in vivo tear sampling from rabbits. The microbiological assay showed 5 days of ERY release in the tear fluid for the observed formulations. Although all formulations showed promising pharmacokinetics to be used as ocular inserts, the formula-



tion prepared by CD- $\beta$  as the matrix component showed higher mucoadhesion, AUC<sub>0–120</sub> and MRT among formulations, and hence can be selected as the optimized formulation. The in vivo testing test showed no significant signs of ocular irritation. Finally, it could be concluded that the ERY-loaded EUD/PVA nanoparticles incorporated into ocular films can be considered a promising ocular formulation for the extended-release of ERY. Patient compliance can be potentially enhanced using the developed inserts, where there is less need for frequent administration compared to the conventional ointment. The authors believed that these formulations have the potential to be further developed and evaluated for delivery of various topical ocular agents such as antibiotics, antifungals, ocular hypotensive, steroids and nonsteroidal anti-inflammatory, antihistamines, decongestants etc., but to prove their usefulness for a particular clinical indication systematic study should be performed.

**Author Contributions:** Conceptualization, S.M.; methodology, S.M.; software, S.M. and S.T.; validation, A.N. and S.M.; formal analysis, A.N., S.T. and S.M.; investigation, S.T. and S.M.; resource, S.M., A.N. and R.G.A.; data curation, A.N., R.G.A. and S.M.; writing—original draft preparation, S.M., R.G.A. and A.N.; writing—review and editing, S.M., R.G.A. and A.N.; supervision, S.M., R.G.A. and A.N.; project administration, S.M. and A.N.; funding acquisition, S.M. All authors have read and agreed to the published version of the manuscript.

**Funding:** This research was funded by Kermanshah University of Medical Sciences with the grant number of 97488.

**Institutional Review Board Statement:** All experiments were approved by the Institutional Animal Ethics Committee (approval number: IR.KUMS.REC.1397.406) of Kermanshah University of Medical Sciences (Kermanshah, Iran).

**Informed Consent Statement:** Not applicable.

**Data Availability Statement:** Data will be sent to the applicants after sending their requests to the corresponding author. The applicants will need to sign a data access agreement.

**Acknowledgments:** The authors faithfully thank Rahesh Daru Novin Co. for cooperation in providing materials and equipment.

**Conflicts of Interest:** The authors declare that they have no conflict of interest.

## References

1. Bhattacharjee, A.; Das, P.J.; Adhikari, P.; Marbaniang, D.; Pal, P.; Ray, S.; Mazumder, B. Novel drug delivery systems for ocular therapy: With special reference to liposomal ocular delivery. *Eur. J. Ophthalmol.* **2019**, *29*, 113–126. [[CrossRef](#)]
2. Gaudana, R.; Ananthula, H.K.; Parenky, A.; Mitra, A.K. Ocular drug delivery. *AAPS J.* **2010**, *12*, 348–360. [[CrossRef](#)] [[PubMed](#)]
3. Gilhotra, R.M.; Nagpal, K.; Mishra, D.N. Azithromycin novel drug delivery system for ocular application. *Int. J. Pharm. Investig.* **2011**, *1*, 22–28. [[CrossRef](#)] [[PubMed](#)]
4. Patel, A.; Cholkar, K.; Agrahari, V.; Mitra, A.K. Ocular drug delivery systems: An overview. *World J. Pharmacol.* **2013**, *2*, 47–64. [[CrossRef](#)] [[PubMed](#)]
5. Ahuja, A.; Khar, R.K.; Ali, J. Mucoadhesive drug delivery systems. *Drug Dev. Ind. Pharm.* **1997**, *23*, 489–515. [[CrossRef](#)]
6. Del Amo, E.M.; Urtti, A. Current and future ophthalmic drug delivery systems. A shift to the posterior segment. *Drug Discov. Today* **2008**, *13*, 135–143. [[CrossRef](#)]
7. Le Boursais, C.; Acar, L.; Zia, H.; Sado, P.A.; Needham, T.; Leverage, R. Ophthalmic drug delivery systems—Recent advances. *Prog. Retin. Eye Res.* **1998**, *17*, 33–58. [[CrossRef](#)]
8. Mehrandish, S.; Mirzaeei, S. A Review on Ocular Novel Drug Delivery Systems of Antifungal Drugs: Functional Evaluation and Comparison of Conventional and Novel Dosage Forms. *Adv. Pharm. Bull.* **2021**, *11*, 28–38. [[CrossRef](#)]
9. Mirzaeei, S.; Berenjian, K.; Khazaei, R. Preparation of the Potential Ocular Inserts by Electrospinning Method to Achieve the Prolong Release Profile of Triamcinolone Acetonide. *Adv. Pharm. Bull.* **2018**, *8*, 21–27. [[CrossRef](#)]
10. Taghe, S.; Mirzaeei, S. Preparation and characterization of novel, mucoadhesive ofloxacin nanoparticles for ocular drug delivery. *Braz. J. Pharm. Sci.* **2019**, *55*, e17105. [[CrossRef](#)]
11. Soppimath, K.S.; Aminabhavi, T.M.; Kulkarni, A.R.; Rudzinski, W.E. Biodegradable polymeric nanoparticles as drug delivery devices. *J. Control. Release* **2001**, *70*, 1–20. [[CrossRef](#)]
12. Mitchell, M.J.; Billingsley, M.M.; Haley, R.M.; Wechsler, M.E.; Peppas, N.A.; Langer, R. Engineering precision nanoparticles for drug delivery. *Nat. Rev. Drug Discov.* **2021**, *20*, 101–124. [[CrossRef](#)] [[PubMed](#)]

13. Kumari, A.; Yadav, S.K.; Yadav, S.C. Biodegradable polymeric nanoparticles based drug delivery systems. *Colloids Surf. B Biointerfaces* **2010**, *75*, 1–18. [[CrossRef](#)] [[PubMed](#)]
14. Nagarwal, R.C.; Kant, S.; Singh, P.N.; Maiti, P.; Pandit, J.K. Polymeric nanoparticulate system: A potential approach for ocular drug delivery. *J. Control. Release* **2009**, *136*, 2–13. [[CrossRef](#)]
15. Zhou, H.Y.; Hao, J.L.; Wang, S.; Zheng, Y.; Zhang, W.S. Nanoparticles in the ocular drug delivery. *Int. J. Ophthalmol.* **2013**, *6*, 390–396. [[CrossRef](#)]
16. Hermans, K.; Van den Plas, D.; Kerimova, S.; Carleer, R.; Adriaensens, P.; Weyenberg, W.; Ludwig, A. Development and characterization of mucoadhesive chitosan films for ophthalmic delivery of cyclosporine A. *Int. J. Pharm.* **2014**, *472*, 10–19. [[CrossRef](#)]
17. Khutoryanskaya, O.V.; Morrison, P.W.; Seilkhanov, S.K.; Mussin, M.N.; Ozhmukhametova, E.K.; Rakhypbekov, T.K.; Khutoryanskiy, V.V. Hydrogen-bonded complexes and blends of poly(acrylic acid) and methylcellulose: Nanoparticles and mucoadhesive films for ocular delivery of riboflavin. *Macromol. Biosci.* **2014**, *14*, 225–234. [[CrossRef](#)]
18. Mohammadi, G.; Mirzaeei, S.; Taghe, S.; Mohammadi, P. Preparation and Evaluation of Eudragit® L100 Nanoparticles Loaded Impregnated with KT Tromethamine Loaded PVA-HEC Insertions for Ophthalmic Drug Delivery. *Adv. Pharm. Bull.* **2019**, *9*, 593–600. [[CrossRef](#)]
19. Querengesser, E.I.; Ormsby, H.L. Ocular penetration of erythromycin. *Can. Med. Assoc. J.* **1955**, *72*, 200–202.
20. Naib, K.; Hallett, J.W.; Leopold, I.H. Observations on the ocular effects of erythromycin. *Am. J. Ophthalmol.* **1955**, *39*, 395–399. [[CrossRef](#)]
21. Freidlin, J.; Acharya, N.; Lietman, T.M.; Cevallos, V.; Whitcher, J.P.; Margolis, T.P. Spectrum of eye disease caused by methicillin-resistant *Staphylococcus aureus*. *Am. J. Ophthalmol.* **2007**, *144*, 313–315. [[CrossRef](#)] [[PubMed](#)]
22. Hammerschlag, M.R.; Chandler, J.W.; Alexander, E.R.; English, M.; Chiang, W.T.; Koutsky, L.; Eschenbach, D.A.; Smith, J.R. Erythromycin ointment for ocular prophylaxis of neonatal chlamydial infection. *JAMA* **1980**, *244*, 2291–2293. [[CrossRef](#)] [[PubMed](#)]
23. Robert, P.Y.; Adenis, J.P. Comparative review of topical ophthalmic antibacterial preparations. *Drugs* **2001**, *61*, 175–185. [[CrossRef](#)] [[PubMed](#)]
24. Zafar, A.; Imam, S.S.; Yasir, M.; Alruwaili, N.K.; Alsaidan, O.A.; Warsi, M.H.; Mir Najib Ullah, S.N.; Alshehri, S.; Ghoneim, M.M. Preparation of NLCs-Based Topical Erythromycin Gel: In Vitro Characterization and Antibacterial Assessment. *Gels* **2022**, *8*, 116. [[CrossRef](#)] [[PubMed](#)]
25. Verma, D.; Kaul, S.; Jain, N.; Nagaich, U. Fabrication and characterization of ocular phase transition systems for blepharitis: A novel approach. *Drug Deliv. Lett.* **2020**, *10*, 24–37. [[CrossRef](#)]
26. Rasheed, S.H.; Samanvitha, M.; Manjunath, S. Formulation and in-vitro characterization of erythromycin ocular inserts. *Int. J. Res. Pharm. Sci. Tech.* **2020**, *2*, 44–50. [[CrossRef](#)]
27. Bodmeier, R.; Chen, H.; Tyle, P.; Jarosz, P. Spontaneous formation of drug-containing acrylic nanoparticles. *J. Microencapsul.* **1991**, *8*, 161–170. [[CrossRef](#)]
28. Taghe, S.; Mirzaeei, S.; Alany, R.G.; Nokhodchi, A. Polymeric inserts containing Eudragit® L100 nanoparticle for improved ocular delivery of azithromycin. *Biomedicines* **2020**, *8*, 466. [[CrossRef](#)]
29. Mehrandish, S.; Mohammadi, G.; Mirzaeei, S. Preparation and functional evaluation of electrospun polymeric nanofibers as a new system for sustained topical ocular delivery of itraconazole. *Pharm. Dev. Technol.* **2022**, *27*, 25–39. [[CrossRef](#)]
30. Tofighia, P.; Soltani, S.; Montazam, S.H.; Montazam, S.A.; Jelvehgari, M. Formulation of tolmetin ocusers as carriers for ocular drug delivery system. *Iran. J. Pharm. Res.* **2017**, *16*, 432–441.
31. Mustafa, W.W.; Fletcher, J.; Khoder, M.; Alany, R.G. Solid Dispersions of Gefitinib Prepared by Spray Drying with Improved Mucoadhesive and Drug Dissolution Properties. *AAPS PharmSciTech* **2022**, *4*, 48. [[CrossRef](#)] [[PubMed](#)]
32. Thrimawithana, T.R.; Young, A.; Buntac, C.R.; Greend, C.R.; Alany, R.G. In-vitro and in-vivo evaluation of carrageenan/methylcellulose polymeric systems for transscleral delivery of macromolecules. *Eur. J. Pharm. Sci.* **2011**, *44*, 399–409. [[CrossRef](#)]
33. Sabbagh, F.; Kiarostami, K.; Mahmoudi Khatir, N.; Rezaia, S.; Muhamad, I.I. Green Synthesis of Mg<sub>0.99</sub>Zn<sub>0.01</sub>O Nanoparticles for the Fabrication of  $\kappa$ -Carrageenan/NaCMC Hydrogel in order to Deliver Catechin. *Polymers* **2020**, *12*, 861. [[CrossRef](#)] [[PubMed](#)]
34. Rattanapoltaveechai, R.; Vongkom, W.; Suntornsuk, W.; Suntornsuk, L. Simple and rapid spectrophotometric method for the analysis of erythromycin in pharmaceutical dosage forms. *J. Food Drug Anal.* **2007**, *15*, 10–14. [[CrossRef](#)]
35. Griessmann, K.; Kaunzinger, A.; Schubert-Zsilavec, M.; Abdel-Tawab, M. A rapid HPLC-UV method for the quantification of erythromycin in dermatological preparations. *Pharmazie* **2007**, *62*, 668–671.
36. Queiroz, K.M.; Silva, M.-L.M.; Prado, N.D.; Lima, P.M.A.; Diniz, R.D.L.; César, I.C.; Pianetti, G.A.; Santos, D.A. Comparison of microbiological assay and HPLC-UV for determination of fluconazole in capsules. *Braz. J. Pharm. Sci.* **2009**, *45*, 693–700. [[CrossRef](#)]
37. Bahrami, G.; Mirzaeei, S.; Kiani, A. High performance liquid chromatographic determination of azithromycin in serum using fluorescence detection and its application in human pharmacokinetic studies. *J. Chromatogr. B* **2005**, *820*, 277–281. [[CrossRef](#)] [[PubMed](#)]
38. Cháfer-Pericás, C.; Maquieira, Á.; Puchades, R. Fast screening methods to detect antibiotic residues in food samples. *Trends Anal. Chem.* **2010**, *29*, 1038–1049. [[CrossRef](#)]
39. Diebold, Y.; Jarrín, M.; Sáez, V.; Carvalho, E.L.; Orea, M.; Calonge, M.; Seijo, B.; Alonso, M.J. Ocular drug delivery by liposome-chitosan nanoparticle complexes (LCS-NP). *Biomaterials* **2007**, *28*, 1553–1564. [[CrossRef](#)]

40. Schopf, L.R.; Popov, A.M.; Enlow, E.M.; Bourassa, J.L.; Ong, W.Z.; Nowak, P.; Chen, H. Topical ocular drug delivery to the back of the eye by mucus-penetrating particles. *Transl. Vis. Sci. Technol.* **2015**, *4*, 11. [[CrossRef](#)]
41. Gagandeep; Garg, T.; Malik, B.; Rath, G.; Goyal, A.K. Development and characterization of nano-fiber patch for the treatment of glaucoma. *Eur. J. Pharm. Sci.* **2014**, *53*, 10–16. [[CrossRef](#)] [[PubMed](#)]
42. Sun, X.; Yu, Z.; Cai, Z.; Yu, L.; Lv, Y. Voriconazole composited polyvinyl alcohol/hydroxypropyl- $\beta$ -cyclodextrin nanofibers for ophthalmic delivery. *PLoS ONE* **2016**, *11*, e0167961. [[CrossRef](#)] [[PubMed](#)]
43. Hao, S.; Wang, B.; Wang, Y.; Zhu, L.; Wang, B.; Guo, T. Preparation of Eudragit L 100-55 enteric nanoparticles by a novel emulsion diffusion method. *Colloids Surf. B Biointerfaces* **2013**, *108*, 127–133. [[CrossRef](#)]
44. Cetin, M.; Atila, A.; Kadioglu, Y. Formulation and in vitro characterization of Eudragit<sup>®</sup> L100 and Eudragit<sup>®</sup> L100-PLGA nanoparticles containing diclofenac sodium. *AAPS PharmSciTech* **2010**, *11*, 1250–1256. [[CrossRef](#)]
45. Tuncay, M.; Calis, S.; Kas, H.S.; Ercan, M.T.; Peksoy, I.; Hincal, A.A. Diclofenac sodium incorporated PLGA (50:50) microspheres: Formulation considerations and in vitro/in vivo evaluation. *Int. J. Pharm.* **2000**, *195*, 179–188. [[CrossRef](#)]
46. Terreni, E.; Chetoni, P.; Burgalassi, S.; Tampucci, S.; Zucchetti, E.; Chipala, E.; Alany, R.G.; Al-Kinani, A.A.; Monti, D. A hybrid ocular delivery system of cyclosporine-A comprising nanomicelle-laden polymeric inserts with improved efficacy and tolerability. *Biomater. Sci.* **2021**, *9*, 8235–8248. [[CrossRef](#)]
47. Glasser, W.G. 6. Prospects for future applications of cellulose acetate. In Proceedings of the Macromolecular Symposia, Weinheim, Germany, 21 April 2004; pp. 371–394.
48. Zong, X.; Kim, K.; Fang, D.; Ran, S.; Hsiao, B.S.; Chu, B. Structure and process relationship of electrospun bioabsorbable nanofiber membranes. *Polymer* **2002**, *43*, 4403–4412. [[CrossRef](#)]
49. Kumari, A.; Sharma, P.K.; Garg, V.K.; Garg, G. Ocular inserts—Advancement in therapy of eye diseases. *J. Adv. Pharm. Technol. Res.* **2010**, *1*, 291–296. [[CrossRef](#)]
50. Bodor, N.; Buchwald, P. Ophthalmic drug design based on the metabolic activity of the eye: Soft drugs and chemical delivery systems. *AAPS J.* **2005**, *7*, E820–E833. [[CrossRef](#)]
51. Mishra, D.; Gilhotra, R. Design and characterization of bioadhesive in-situ gelling ocular inserts of gatifloxacin sesquihydrate. *DARU J. Pharm. Sci.* **2008**, *16*, 1–8.
52. Sharma, S.; Mohanty, S.; Gupta, D.; Jassal, M.; Agrawal, A.K.; Tandon, R. Cellular response of limbal epithelial cells on electrospun poly-epsilon-caprolactone nanofibrous scaffolds for ocular surface bioengineering: A preliminary in vitro study. *Mol. Vis.* **2011**, *17*, 2898–2910.
53. Parveen, S.; Chaudhury, P.; Dasmahapatra, U.; Dasgupta, S. Biodegradable protein films from gallic acid and the cataractous eye protein isolate. *Int. J. Biol. Macromol.* **2019**, *139*, 12–20. [[CrossRef](#)] [[PubMed](#)]
54. Tanwar, Y.; Patel, D.; Sisodia, S. In vitro and in vivo evaluation of ocular inserts of ofloxacin. *DARU J. Pharm. Sci.* **2007**, *15*, 139–145.
55. Wibowo, A.C.; Misra, M.; Park, H.-M.; Drzal, L.T.; Schalek, R.; Mohanty, A.K. Biodegradable nanocomposites from cellulose acetate: Mechanical, morphological, and thermal properties. *Compos. Part A Appl. Sci. Manuf.* **2006**, *37*, 1428–1433. [[CrossRef](#)]
56. Anirudhan, T.S.; Mohan, A.M. Novel pH sensitive dual drug loaded-gelatin methacrylate/methacrylic acid hydrogel for the controlled release of antibiotics. *Int. J. Biol. Macromol.* **2018**, *110*, 167–178. [[CrossRef](#)] [[PubMed](#)]
57. Rathod, L.V.; Kapadia, R.; Sawant, K.K. A novel nanoparticles impregnated ocular insert for enhanced bioavailability to posterior segment of eye: In vitro, in vivo and stability studies. *Mater. Sci. Eng. C Mater. Biol. Appl.* **2017**, *71*, 529–540. [[CrossRef](#)]
58. Adhikari, R.P.; Shrestha, S.; Barakoti, A.; Amatya, R. Inducible clindamycin and methicillin resistant Staphylococcus aureus in a tertiary care hospital, Kathmandu, Nepal. *BMC Infect. Dis.* **2017**, *17*, 483. [[CrossRef](#)]
59. Tereshchenkov, A.; Shishkina, A.; Karpenko, V.; Chertkov, V.; Konevega, A.; Kasatsky, P.; Bogdanov, A.; Sumbatyan, N. New fluorescent macrolide derivatives for studying interactions of antibiotics and their analogs with the ribosomal exit tunnel. *Biochemistry* **2016**, *81*, 1163–1172. [[CrossRef](#)] [[PubMed](#)]
60. Hedges, A. Cyclodextrins: Properties and applications. In *Starch*; Elsevier: Amsterdam, The Netherlands, 2009; pp. 833–851.
61. Gokce, E.H.; Sandri, G.; Bonferoni, M.C.; Rossi, S.; Ferrari, F.; Güneri, T.; Caramella, C. Cyclosporine A loaded SLNs: Evaluation of cellular uptake and corneal cytotoxicity. *Int. J. Pharm.* **2008**, *364*, 76–86. [[CrossRef](#)]
62. Driot, J.-Y.; Novack, G.D.; Rittenhouse, K.D.; Milazzo, C.; Pearson, A.P. Ocular pharmacokinetics of fluocinolone acetonide after Retisert<sup>™</sup> intravitreal implantation in rabbits over a 1-year period. *J. Ocul. Pharmacol. Ther.* **2004**, *20*, 269–275. [[CrossRef](#)]
63. Ghate, D.; Edelhauser, H.F. Ocular drug delivery. *Expert Opin. Drug Deliv.* **2006**, *3*, 275–287. [[CrossRef](#)] [[PubMed](#)]
64. Chhonker, Y.S.; Prasad, Y.D.; Chandasana, H.; Vishvkarma, A.; Mitra, K.; Shukla, P.K.; Bhatta, R.S. Amphotericin-B entrapped lecithin/chitosan nanoparticles for prolonged ocular application. *Int. J. Biol. Macromol.* **2015**, *72*, 1451–1458. [[CrossRef](#)] [[PubMed](#)]
65. Mirzaeei, S.; Taghe, S.; Asare-Addo, K.; Nokhodchi, A. Polyvinyl Alcohol/Chitosan Single-Layered and Polyvinyl Alcohol/Chitosan/Eudragit RL100 Multi-layered Electrospun Nanofibers as an Ocular Matrix for the Controlled Release of Ofloxacin: An In Vitro and In Vivo Evaluation. *AAPS PharmSciTech* **2021**, *22*, 170. [[CrossRef](#)] [[PubMed](#)]